Measurements of Collective Collapse in a Bose-Einstein Condensate with Attractive Interactions

C. A. Sackett, J. M. Gerton, M. Welling, and R. G. Hulet
Physics Department and Rice Quantum Institute, Rice University, Houston, Texas 77251
(Received 23 July 1998)

The occupation number of a magnetically trapped Bose-Einstein condensate is limited for atoms with attractive interactions. It has been predicted that, as this limit is approached, the condensate will collapse by a collective process. The measured spread in condensate number for samples of ^{7}Li atoms undergoing thermal equilibration is consistent with the occurrence of such collapses. [S0031-9007(98)08366-5]

PACS numbers: 03.75.Fi, 32.80.Pj

The attainment of Bose-Einstein condensation (BEC) in dilute atomic gases has provided a new domain for studying the nonlinear effects of interactions in thermodynamic systems. Among the gases in which BEC has been observed, ^{7}Li is unique in having a negative triplet s-wave scattering length a. Because $a < 0$, the effective interaction between atoms is attractive, and the BEC phenomenon is substantially altered. Attractive interactions were long believed to make a condensate unstable and thus prevent BEC [1,2], but it is now known that, for a confined gas, a metastable condensate can exist as long as its occupation number, N_0, remains small [3]. Such condensates are predicted to be rich in physics, exhibiting properties such as solitonlike behavior [4] and macroscopic quantum tunneling [5]. In particular, complex dynamical behavior is expected as N_0 approaches its stability limit [6–8]. In this Letter, we describe experimental investigations of this behavior.

Attractive interactions limit N_0 because, at a maximum number N_m, the compressibility of the condensate becomes negative and it will implosively collapse. By equating the positive zero-point kinetic energy to the negative interaction energy, it is found that $N_m \sim \ell/|a|$ when the condensate is confined to volume ℓ^3. The stability limit is more precisely determined from numerical solution of the nonlinear Schrödinger equation (NLSE) [9]. For ^{7}Li in our magnetic trap, $a = -1.46$ nm [10] and $\ell \approx 3$ μm, which yield a stability limit of $\sim$1250 atoms.

As the gas is cooled below the critical temperature for BEC, N_0 grows until N_m is reached. The condensate then collapses spontaneously if $N_0 \geq N_m$, or the collapse can be initiated by thermal fluctuations or quantum tunneling for $N_0 \lesssim N_m$ [5,7]. During the collapse, the condensate shrinks on the time scale of the trap oscillation period. As the density rises, the rates for inelastic collisions such as dipolar decay and three-body molecular recombination increase. These processes release sufficient energy to immediately eject the colliding atoms from the trap, thus reducing N_0. The ejected atoms are very unlikely to further interact with the gas before leaving the trap, since the density of noncondensed atoms is low. As the collapse proceeds, the collision rate grows quickly enough that the density remains small compared to $|a|^{-3}$ and the condensate remains a dilute gas [7,8].

Both the collapse and the initial cooling process displace the gas from thermal equilibrium. As long as N_0 is smaller than its equilibrium value, as determined by the total number and average energy of the trapped atoms, the condensate will continue to fill until another collapse occurs. This cycle of condensate growth and collapse repeats until the gas comes to equilibrium with $N_0 < N_m$. We have modeled the equilibration process by numerical solution of the quantum Boltzmann equation (QBE) [7]. Figure 1 shows three possible trajectories of N_0 in time, for our experimental conditions. The differences arise from the stochastic collapse initiation process and from modeled variations in the experiment. Although theories are not yet conclusive as to what fraction of the condensate atoms is

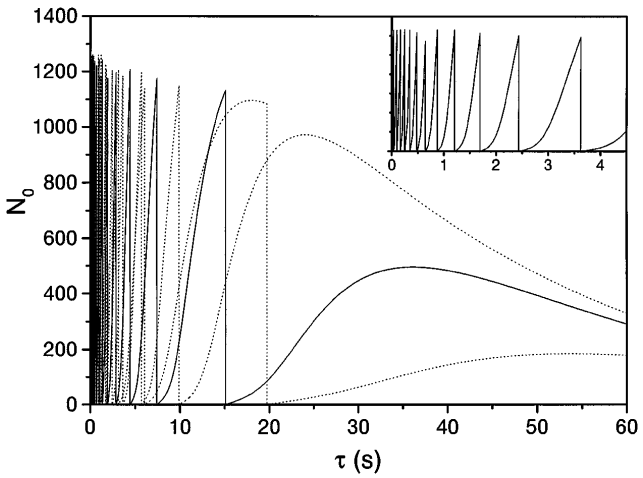

FIG. 1. Numerical solutions of the quantum Boltzmann equation, showing evolution of condensate occupation number. A trapped, degenerate ^{7}Li gas is quenched at $\tau = 0$ to a temperature of $T \approx 100$ nK and a total number of $N \approx 4 \times 10^4$ atoms. The gas then freely evolves in time. The differences in the traces reflect experimental variations in cooling and the stochastic nature of the collapse initiation process. The inset shows an expanded view of one of the traces at early times, on the same vertical scale.

 0031-9007/99/82(5)/876(4)$15.00

lost in the collapse, we assume here that N_0 is reduced to zero [7].

The apparatus used to produce BEC has been described previously [6]. Approximately 10^8 laser-cooled ^{7}Li atoms are loaded into a permanent magnet trap. The gas is then evaporatively cooled into the degenerate regime using an applied microwave field that ends at a microwave frequency 100 kHz above the trap bottom, leaving a total number $N \approx 4 \times 10^5$ atoms at a temperature $T \approx 400$ nK. The frequency is then rapidly reduced to $\sim$10 kHz and raised again, leaving approximately 4×10^4 atoms. By sweeping the frequency fast compared to the collision rate, all atoms above the cutoff energy are simply eliminated and a definite energy distribution is created at a specified time. Reducing N also enables the condensate to be more accurately distinguished from the noncondensed cloud.

The atoms are observed by illuminating the cloud with an off-resonant laser beam and imaging the coherently scattered light onto a CCD camera using the polarization phase contrast technique described in Refs. [6,11]. The resulting signal is fit to determine N_0. Because the gas is not in equilibrium, it does not obey the ordinary Bose-Einstein energy distribution function. The QBE model predicts that, within a few collision times after the microwave sweep, the distribution becomes locally equilibrated, in the sense that it can be described by an equilibrium distribution with an effective chemical potential that varies slowly as a function of energy. The distributions calculated in the model can be simply and accurately parametrized as

$$f(E) = \frac{\exp[\beta(\mu_1 - \mu_2)]}{\exp[\beta(E - \mu_2)] - 1} \equiv \frac{A}{\exp[\beta(E - \mu_2)] - 1}, \quad (1)$$

where E is the energy of a level. At high energies, f has the form of a Boltzmann distribution with chemical potential μ_1 and temperature β^{-1}, while at low energies f has the form $A f_{\mathrm{BE}}(\mu_2, \beta)$, where f_{BE} is the equilibrium Bose-Einstein distribution and $A = \exp(\beta \Delta\mu)$ is a constant. Generally, μ_2 lies just below the ground state energy, and $\Delta\mu$ is positive with A in the range of 1–10, indicating that there is an excess of high-energy atoms during equilibration.

Equation (1) is fit to image data in order to determine μ_2, β, and A, following the procedure outlined in Ref. [6]. Good agreement is generally observed, lending confidence to the choice of f. Systematic errors introduced by the nonequilibrium model are estimated by applying the fitting procedure to simulated data generated by the QBE, and also by comparing the analysis of experimental images of thermalized clouds using both equilibrium and nonequilibrium models. These tests indicate the uncertainty to be $\sim$75 atoms. More significant than this is the uncertainty introduced by imaging limitations. The imaging system is nearly diffraction limited, but the resolution is comparable to the size of the condensate and so must be taken into account [12]. The imaging system consists of the lenses described in Ref. [6] with an additional custom corrective lens to reduce spherical aberrations. The system was tested and characterized on the bench by imaging laser light emitted from an optical fiber, but uncertainty arises in use because of possible focusing errors and aberrations from the vacuum viewport through which the trap is observed. This uncertainty can be estimated from the size and location of ripples in images of degenerate clouds caused by imaging imperfections. If the lens parameters used in the imaging model are adjusted to reproduce these ripples, the values of N_0 increase by 40% over those obtained using the parameters measured on the bench [13]. We therefore estimate our systematic uncertainty to be $\pm 20\%$, and report values calculated using the average lens parameters.

Although phase-contrast imaging can, in principle, be nearly nonperturbative, it is necessary to scatter several photons per atom during the probe pulse in order to measure N_0 with the required accuracy. This heats the gas and precludes the possibility of directly observing the evolution of N_0 in time as in Fig. 1. This limitation cannot be overcome by repeating the experiment and varying the delay time τ between the microwave sweep and the probe, because the evolution of N_0 is made unrepeatable by random thermal and quantum fluctuations in the condensate growth and collapse, as well as experimental fluctuations in the initial conditions. These fluctuations are expected to cause the values of N_0 to vary from one repetition to the next, as seen in Fig. 1. We observe such variations, and show their measured distribution for several values of τ in Fig. 2. For small τ, N_0 ranges from near zero to about 1200 atoms, as expected if the condensate is continually filling to the theoretical maximum and collapsing.

To our knowledge, no other fundamental explanation for variations of this magnitude has been proposed, so we believe that these measurements strongly support the collapse/fill model. Much care has been taken to investigate sources of experimental noise which might cause the measured values of N_0 to vary. The systematic errors discussed above do not contribute to the variations, since all of the images used to generate Fig. 2 were analyzed in the same way. However, shot noise in the camera is a source of statistical uncertainty which results in a spread in measured values. The noise level is determined by observing images of an empty trap. Using the measured shot noise, the fits give average values of reduced χ^2 of very nearly one. The statistical uncertainty in N_0 is determined to be ± 60 atoms, by finding the change required to increase by one the unreduced value of χ^2 [14]. This uncertainty is consistent with the values obtained for $\tau = 90$ s, when N_0 is expected to be small. At short τ, the rms variation in the observed values is 250 atoms, much larger than the uncertainty due to shot noise. Note that some bias is introduced since the nonequilibrium model never allows $N_0 < 0$.

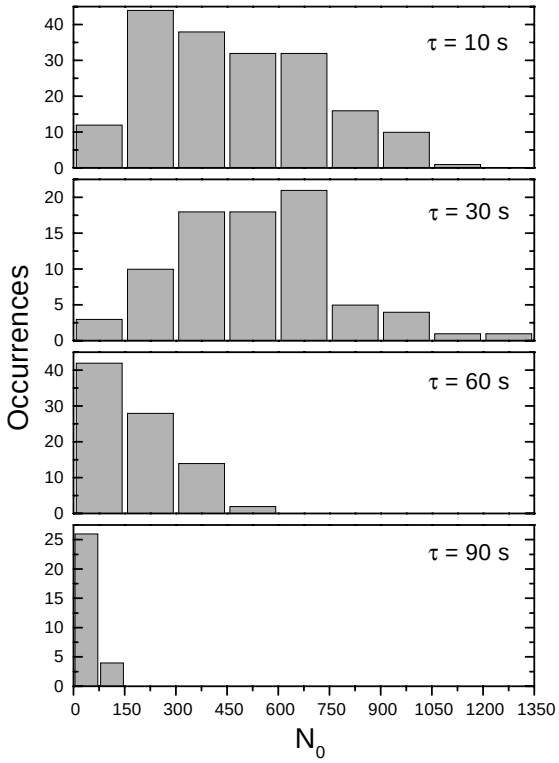

FIG. 2. Frequency of occurrence of condensate occupation number. For each measurement, a nonequilibrium degenerate gas was produced, allowed to evolve freely for time τ, and then probed. The total number of trapped atoms at each τ ranged from 5×10^3 to 3.5×10^4. A histogram was also constructed for $\tau = 5$ s, and found to be very similar to the $\tau = 10$ s data.

Because of this, values of the lowest bin in the histograms will be somewhat increased.

The observed variations might also be caused by other uncontrolled experimental fluctuations. Indeed, the total number of atoms observed in the trap is found to vary by $\sim 10^4$ atoms from one repetition to the next, so experimental fluctuations are significant. However, if the variations in N_0 were caused by such an effect, the measured values should be correlated with those of the responsible parameter. Contingency-square analysis [14] was used to determine that no statistically significant correlation exists with changes in N, T, phase-space density, loading conditions, evaporative cooling trajectory, probe parameters, goodness of fit, or from one measurement and the next. We therefore conclude that the variations are, in fact, intrinsic to the gas and reflect the underlying dynamical behavior.

The histograms can be compared with the predictions of the QBE. In Fig. 1, three time domains can be discerned. For $\tau \leq 20$ s, the condensate collapses frequently as the gas is equilibrating. Experimental results at $\tau = 5$ and 10 s are very similar, and agree qualitatively with the model prediction in being broadly spread between 0 and N_m. Around $\tau = 20$–50 s, equilibrium is reached and N_0 is stabilized for several seconds at a value which depends sensitively on the details of the trajectory. At later times, N_0 declines as atoms are lost through inelastic collisions.

The detailed shape of the model histogram for $\tau \leq 20$ s can be understood from the dependence of N_0 on time as the condensate fills, since the probability of observing a particular N_0 value is proportional to $(dN_0/dt)^{-1}$ at that N_0 value. After a collapse, the condensate initially fills slowly because the Bose enhancement factor is small. Subsequently, the growth rate increases until N_0 reaches ~ 100 atoms, when the growth becomes linear. This saturation occurs as the populations of low-lying energy levels in the trap become depleted. Condensate growth is then limited by the rate for collisions between high-energy atoms to produce more low-energy atoms, which yields a constant fill rate. Because of these effects, a histogram calculated under the assumption that the collapse drives $N_0 \rightarrow 0$ is significantly peaked at small N_0, and lower but flat between $N_0 = 100$ and N_m.

The observed histogram differs quantitatively from this prediction in several respects. There is no peak observed at low N_0; rather, a broad peak occurs at $N_0 = 200$–700 atoms. This suggests that the condensate does not collapse to zero atoms, but the fact that some clouds with $N_0 \simeq 50$ atoms are observed then indicates that the condensate collapses to a range of final values. Kagan *et al.* have observed the condensate to collapse to a nonzero value in numerical solutions of the NLSE [8]. However, while those authors found that close to 50% of the condensate was lost, our data suggest that considerably smaller remainders are more likely, since a large fraction of our observations show $N_0 < 600$ atoms.

We also observe the frequency of occurrence to drop steadily as N_0 increases, rather than remaining flat up to $N_0 = N_m$ as predicted. This observation might be explained in either of two ways. If the condensate growth does not saturate but continues to accelerate, then the probability of observing large N_0 values would decrease. This might result from the depression of the condensate energy by mean-field interactions, which are not included in the QBE. Alternatively, if the condensate has a larger than expected rate for collapsing at relatively low N_0, then the probability of condensates surviving to large N_0 would decrease. This might be possible if the condensate is typically in a more excited state than expected from the temperature of the gas. Kagan *et al.* predict such excitations to occur during the growth and collapse processes, but quantitative estimates of the effect under our experimental conditions are not yet available.

Quantitative comparison of theory and experiment is more difficult at longer τ, since dN_0/dt then depends sensitively on the time of the last collapse, as seen in Fig. 1. The numerical results obtained are consistent with the measured distribution at $\tau = 30$ s, but give somewhat higher N_0 values than observed at $\tau = 60$ and 90 s. This may be due to technical sources of heating not included in the simulation.

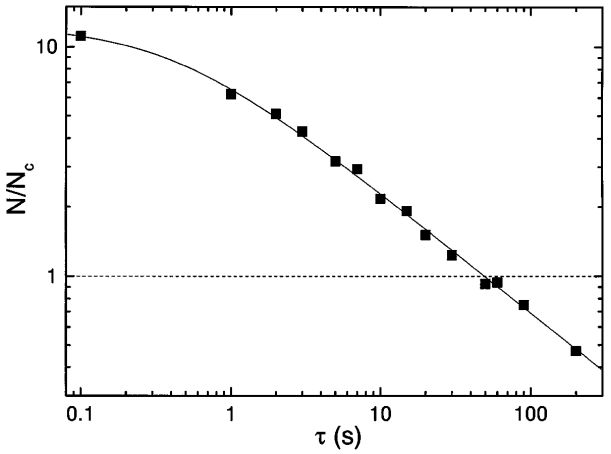

FIG. 3. Relaxation of degenerate gas to equilibrium. Data were taken as in Fig. 2, but for each image the fitted values of N and β were used to determine N/N_c, where $N_c = 1.2(\hbar\omega\beta)^{-3}$. At each τ, the microwave sweep was adjusted to maintain N at approximately 2×10^4 atoms to agree with the ranges used in Fig. 2. The solid curve is a fit to the empirical form $\alpha(1 + \kappa\tau)^{\gamma}$, yielding $\alpha = 12.5$, $\kappa = 2.5\ \mathrm{s}^{-1}$, and $\gamma = -0.52$. Note that the significance of the point at $\tau = 60$ s having $N/N_c < 1$ is low, due to the statistical and systematic errors described in the text. It is therefore consistent with Fig. 2 which shows some measurements with $N_0 \gg 1$.

The condensate growth and collapse cycle is driven by an excess of noncondensed atoms compared to a thermal distribution. This excess can be examined directly. From N and the temperature parameter β, the critical number for the BEC transition, N_c, is calculated and the ratio N/N_c plotted as a function of τ in Fig. 3. The points represent averages of several measurements; at each τ a spread of $\sim$40% in N/N_c was observed. In addition, systematic errors limit the accuracy of the values to $\sim$30% at early times, but once $N/N_c \sim 1$, the images are fit to equilibrium distributions and the error is reduced to $\sim$10%.

Since $N_m \ll N$, equilibrium is reached when $N/N_c \approx 1$, which occurs when $\tau \approx 50$ s, a time long compared to the elastic collision time scale of $\sim$1 s. This suggests that growth of the condensate is a significant bottleneck when N_0 is constrained to be relatively small. Similar behavior is observed in the QBE calculation. The time scale for equilibration is the same as that of the changing shape of the histograms in Fig. 2, which further strengthens the conclusion that the variations in N_0 are related to condensate dynamics, since the distribution changes at approximately the same time that the population imbalance driving condensate growth is eliminated.

We believe that the observations reported here are the first indicator of the complex dynamics accompanying BEC in a gas with attractive interactions, and that they support the collective collapse/fill model as a useful framework for considering such systems. At the same time, they point out the need for more accurate theoretical simulations which can quantitatively reproduce the observed variations in N_0. Naturally, an accurate, nonperturbative and continuous measurement of N_0 in time would be a more decisive experiment, but such a measurement is unfortunately not achievable given the low value of N_m. We therefore expect that our observations, though indirect, will help to further our understanding of this novel and interesting state of matter.

We thank J. Queneuille and V. Bagnato for providing the corrective lens for our imaging system. We also gratefully acknowledge helpful discussions with H. T. C. Stoof and Yu. Kagan, and funding from the Welch Foundation, NSF, NASA, and ONR.

[1] N. Bogolubov, J. Phys. **XI**, 23 (1947).
[2] H. T. C. Stoof, Phys. Rev. A **49**, 3824 (1994).
[3] C. C. Bradley, C. A. Sackett, and R. G. Hulet, Phys. Rev. Lett. **78**, 985 (1997).
[4] R. J. Dodd *et al.*, Phys. Rev. A **54**, 661 (1996).
[5] Y. Kagan, G. V. Shlyapnikov, and J. T. M. Walraven, Phys. Rev. Lett. **76**, 2670 (1996); E. Shuryak, Phys. Rev. A **54**, 3151 (1996); H. T. C. Stoof, J. Stat. Phys. **87**, 1353 (1997); M. Ueda and A. J. Leggett, Phys. Rev. Lett. **80**, 1576 (1998).
[6] C. A. Sackett, C. C. Bradley, M. Welling, and R. G. Hulet, Appl. Phys. B **65**, 433 (1997).
[7] C. A. Sackett, H. T. C. Stoof, and R. G. Hulet, Phys. Rev. Lett. **80**, 2031 (1998).
[8] Yu. Kagan, A. E. Muryshev, and G. V. Shlyapnikov, Phys. Rev. Lett. **81**, 933 (1998).
[9] P. A. Ruprecht *et al.*, Phys. Rev. A **51**, 4704 (1995); M. Houbiers and H. T. C. Stoof, Phys. Rev. A **54**, 5055 (1996); T. Bergeman, Phys. Rev. A **55**, 3658 (1997).
[10] E. R. I. Abraham, W. I. McAlexander, J. M. Gerton, R. G. Hulet, R. Cote, and A. Dalgarno, Phys. Rev. A **55**, R3299 (1997).
[11] The images described here were taken using a probe detuning of ± 260 MHz, an intensity of 3 $\mathrm{W/cm^2}$, a pulse duration of 6 μs, and an imaging polarizer angle of 82.5° with respect to the probe polarization.
[12] C. C. Bradley, C. A. Sackett, and R. G. Hulet, Phys. Rev. A **55**, 3951 (1997).
[13] The imaging system is characterized by its phase error as a function of aperture radius, ρ. For ρ in cm, the phase error measured on the bench is $\phi = 0.26\rho^2 - 0.36\rho^4 + 0.17\rho^6$ waves, and the phase error derived from experimental images is $\phi = 0.34\rho^2 - 0.30\rho^4 + 0.094\rho^6$ waves.
[14] W. H. Press *et al.*, *Numerical Recipes in C* (Cambridge University Press, Cambridge, England, 1992), 2nd ed.